Structural analysis of the catalytically inactive kinase domain of the human EGF receptor 3

Natalia Jura[a], Yibing Shan[b], Xiaoxian Cao[a], David E. Shaw[b,c], and John Kuriyan[a,d,e,1]

[a]Department of Molecular and Cell Biology and [e]Department of Chemistry, California Institute for Quantitative Biosciences, Howard Hughes Medical Institute, University of California, Berkeley, CA 94720; [d]Physical Biosciences Division, Lawrence Berkeley National Laboratory, Berkeley, CA 94720; [b]D. E. Shaw Research, New York, NY 10036; and [c]The Center for Computational Biology and Bioinformatics, Columbia University, New York, NY 10032

Contributed by John Kuriyan, October 27, 2009 (sent for review September 17, 2009)

The kinase domain of human epidermal growth factor receptor (HER) 3/ErbB3, a member of the EGF receptor (EGFR) family, lacks several residues that are critical for catalysis. Because catalytic activity in EGFR family members is switched on by an allosteric interaction between kinase domains in an asymmetric kinase domain dimer, HER3 might be specialized to serve as an activator of other EGFR family members. We have determined the crystal structure of the HER3 kinase domain and show that it appears to be locked into an inactive conformation that resembles that of EGFR and HER4. Although the crystal structure shows that the HER3 kinase domain binds ATP, we confirm that it is catalytically inactive but can serve as an activator of the EGFR kinase domain. The HER3 kinase domain forms a dimer in the crystal, mediated by hydrophobic contacts between the N-terminal lobes of the kinase domains. This N-lobe dimer closely resembles a dimer formed by inactive HER4 kinase domains in crystal structures determined previously, and molecular dynamics simulations suggest that the HER3 and HER4 N-lobe dimers are stable. The kinase domains of HER3 and HER4 form similar chains in their respective crystal lattices, in which N-lobe dimers are linked together by reciprocal exchange of C-terminal tails. The conservation of this tiling pattern in HER3 and HER4, which is the closest evolutionary homolog of HER3, might represent a general mechanism by which this branch of the HER receptors restricts ligand-independent formation of active heterodimers with other members of the EGFR family.

EGFR | human epidermal growth factor receptor 3 | human epidermal growth factor receptor4 | receptor oligomerization

Members of the epidermal growth factor receptor family of tyrosine kinases (EGFR, also known as HER1 or ErbB1, HER2/ErbB2, HER3/ErbB3, and HER4/ErbB4) undergo ligand-dependent homo- and heterodimerization that results in phosphorylation and the consequent recruitment of other signaling proteins to the sites of receptor activation (1). HER3 is a distinctive member of the EGFR family because its kinase domain lacks certain residues that are known to be essential for catalytic activity in other kinases (2). Phosphorylation of HER3 by other EGFR family members, most commonly by HER2, activates signaling pathways that are indispensable for development (3, 4). Phosphorylated HER3 is a particularly potent signaling molecule because it activates the PI3K/AKT pathway (4, 5). In cancer cells treated with kinase inhibitors such as gefitinb and erlotinib, the diminished activity of HER2 is compensated for by HER3 overexpression, which results in tumor cell survival (3, 6). This partnership between a receptor that lacks a ligand (HER2) and one that lacks kinase activity (HER3) is a unique aspect of the EGFR family but is one that is poorly understood in terms of molecular mechanism.

The activation of EGFR family members involves the formation of asymmetric dimers between their intracellular kinase domains, in which one kinase domain (the activator) acts as an allosteric activator of the other (the receiver) (Fig. 1*A*) (7). This mechanism, in which the activator kinase plays a role analogous to that of a cyclin in the activation of cyclin-dependent kinases (8), helps to explain the importance of HER3 in the activation of EGFR family members. Sequence comparisons suggest that although the kinase domain of HER3 cannot be activated, it can serve as the activator in asymmetric dimers (7).

In this report, we are concerned with the structure of the HER3 kinase domain, for which a crystal structure has not yet been reported. The kinase domain of HER3 shares ~60% sequence identity with the kinase domains of the active members of the EGFR family, but it lacks some of the residues implicated in catalytic activity (e.g., the catalytic base, which is Asp 813 in human EGFR). HER3 has been reported either not to have detectable kinase activity in studies using recombinant protein (2, 9) or to have very low activity when immunoprecipitated from cells (10, 11). Because of the lack of conservation of residues such as the catalytic base, HER3 has been designated as a pseudokinase domain (12). Pseudokinases, which represent ≈10% of all human kinases, are assumed to act as scaffolds or allosteric regulators rather than enzymes and are still relatively poorly characterized as a group. The structures of two pseudokinase domains have been reported so far, those of Ca^{2+}/calmodulin-activated Ser-Thr kinase (CASK) (13) and vaccinia-related kinase 3 (VRK3) (14).

Particularly interesting among the changes in the HER3 sequence relative to its active homologs are those that are localized to helix αC, an important element in kinase regulation. The conformation of helix αC helps to define an inactive conformation that is characteristic of many kinases, including cyclin-dependent kinases (CDKs) (15), Src family kinases (16, 17), Zap70 (18), and EGFR (19). In this inactive conformation, which we refer to as the Src/CDK-like inactive conformation, helix αC is rotated outward with respect to its conformation in the active state and the centrally located activation loop is tightly packed inside the active site in a way that blocks the binding of peptide substrates. On activation, helix αC rotates toward the active site, resulting in an open conformation of the activation loop that is compatible with the binding of substrate peptides (20). In the active conformation, helix αC positions a conserved glutamate residue (Glu 310 in c-Src, Glu 738 in EGFR) so that it can form a salt bridge with a conserved lysine residue that coordinates ATP (Lys 295 in c-Src, Lys 721 in EGFR).

Helix αC plays a special role in EGFR family members by forming part of the docking site on the receiver kinase domain for the activator kinase domain (Fig. 1*B*). The sequence of HER3 in a region spanning helix αC is divergent from that of other EGFR family members (Fig. 1*B*). Glu 738 in EGFR is replaced by histidine in HER3, and residues in EGFR that are important for docking the activator kinase are also not conserved in HER3.

The sequence of HER3 is also divergent in the intracellular juxtamembrane segment, which is critical for stabilization of the

Author contributions: N.J., Y.S., and D.E.S. designed research; N.J., Y.S., and X.C. performed research; N.J., Y.S., D.E.S., and J.K. analyzed data; and N.J. and J.K. wrote the paper.

The authors declare no conflict of interest.

Freely available online through the PNAS open access option.

Data deposition: The data have been deposited in the Protein Data Bank, www.pdb.org (PDB ID codes 3KEX).

[1]To whom correspondence should be addressed. E-mail: kuriyan@berkeley.edu.

This article contains supporting information online at www.pnas.org/cgi/content/full/0912101106/DCSupplemental.

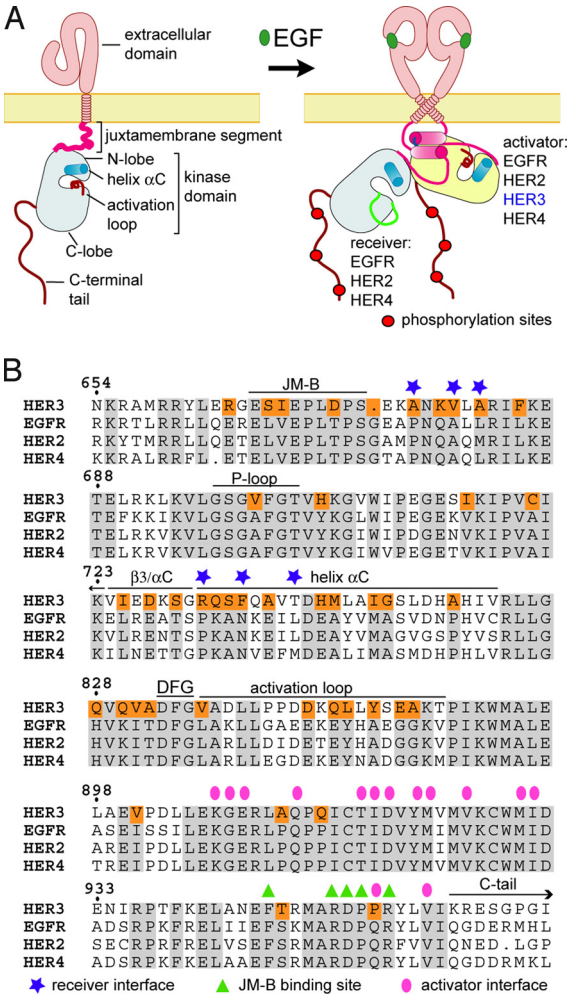

Fig. 1. (*A*) Schematic diagram of EGFR domain structure and the ligand-dependent activation process. (*B*) Multiple sequence alignment of the portions of kinase domains of EGFR family members. The residues that are identical in all four sequences are highlighted in gray, with sequence alterations unique to HER3 highlighted in orange. Residues that are part of the receiver interface are marked by dark blue stars, residues at the activator interface are marked by pink dots, and residues participating in the binding of the JM-B segment are marked by green triangles.

asymmetric dimer (21, 22). The N-terminal portions of the juxtamembrane segment (referred to as JM-A) of the receiver and the activator kinases are likely to interact, and the residues important for this interaction are conserved among the four EGFR family members (21). The C-terminal portion of the juxtamembrane segment (referred to as JM-B) of the receiver kinase interacts with the C-lobe of the activator kinase domain in a latching interaction (21, 22) (Fig. 1*A*). HER3 preserves residues in the C-lobe of the kinase domain that are important for the latching interaction, but the sequence of the JM-B segment is not conserved (Fig. 1*B*). This is consistent with a role for HER3 as a functional activator that cannot serve as a receiver.

Current structural knowledge about HER3 has been limited to its ligand-binding extracellular domains (23). We now present the crystal structure of the kinase domain of the HER3 receptor. We also analyze the catalytic activity of the purified HER3 kinase domain and its ability to activate the EGFR kinase domain. We discuss a potential functional implication of a chain of kinase domains in the HER3 crystal lattice that bears remarkable similarity to chains that are present in crystal structures of HER4 but have not been commented on previously. The formation of these chains is interesting because they would prevent the juxtamembrane segments from participating in asymmetric dimer formation while masking the activating interface of the C-lobe.

Results and Discussion

Structure Determination. We determined the crystal structure of the HER3 kinase domain flanked by a 10-residue portion of the juxtamembrane segment and by a 40-residue portion of the C-terminal tail (residues 674–1,001; the numbering corresponds to the mature HER3 sequence) [supporting information (SI) Table S1]. The crystals were grown in the presence of Mg^{2+} ions, the ATP analogue AMP-PNP, and diffracted x-rays to 2.8 Å. There are two HER3 molecules in the asymmetric unit, and both adopt the Src/CDK inactive conformation (Fig. 2).

Although the conformation of HER3 resembles that of inactive EGFR and HER4 in general terms, there are localized differences centered around helix αC (Fig. 2*B*). These structural changes can be rationalized in terms of a key functional difference in the role of helix αC in active kinases when compared with HER3. In active kinases, including EGFR and HER4, helix αC makes alternative interactions that stabilize it in the inactive (out) conformation as well as in the active (in) conformation (24, 25). In HER3, helix αC appears to be locked in the inactive (out) conformation.

The N-terminal half of helix αC is unwound in HER3, and it forms a well-structured loop connecting helix αC to the preceding β3 strand (Fig. 2*A*). This extended β3/αC loop in HER3 seals off a hydrophobic pocket in the kinase catalytic site. Phe 734 in the β3/αC loop of HER3, which corresponds to an asparagine in active EGFR family members, provides key hydrophobic interactions that stabilize the inactive conformation of the activation loop and helix αC (Fig. 2*B*). The shorter helix αC in HER3 is additionally stabilized by an N-terminal cap provided by Thr 738. In the active EGFR family members, Thr 738 is replaced by bulky hydrophobic residues (Leu in EGFR and HER2, Met in HER4) that are part of the docking site for the activator in the asymmetric dimer interface. In inactive EGFR, the leucine side chain (Leu 736) closes over other hydrophobic side chains and stabilizes the inactive conformation. Thus, a residue that plays a key role in the balance between the inactive (out) and active (in) states of the helix αC in EGFR (Leu 736) is replaced in HER3 by Thr 738, which appears to stabilize the inactive (out) conformation preferentially.

Another key residue in EGFR is Ile 735, which is located in the center of the hydrophobic core formed by Leu 723, Leu 764, and Val 762 in the active conformation. This hydrophobic packing is disrupted in the inactive conformation because of the outward movement of helix αC. The residue corresponding to Ile 735 in HER3, Val 737, is located outside of the shortened helix αC, and the smaller valine side chain in HER3 would be expected to weaken the hydrophobic packing observed in the active conformation of EGFR.

Two key residues that coordinate ATP in the active site, Lys 723 and Asp 833 [in the conserved Asp-Phe-Gly (DFG) motif] are both present in HER3. In addition, the sequence of the P-loop is well conserved. These features are consistent with our observation of strong electron density for the nonhydrolyzable ATP analogue, AMP-PNP (Fig. 2*C*). AMP-PNP is bound in an extended conformation, and its orientation is similar to that seen previously in structures of inactive Src family kinases and EGFR (16, 17, 21). A metal ion is clearly bound in the nucleotide-binding pocket in a manner similar to that observed for inactive EGFR (Fig. 2*C*). Although Mg^{2+} ions were included in the crystallization condition and used in the refinement model, the presence of strong residual electron density (at a level of 4σ above the mean value) in difference maps indicates that the metal is not Mg^{2+} (we have been unable to verify the identity of this metal ion despite considerable effort).

HER3 Can Be a Functional Activator but Not a Receiver Kinase. Because of the unexpected observation of kinase activity for CASK, origi-

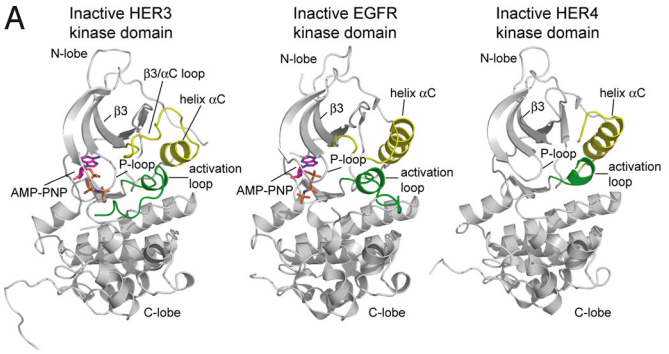

Fig. 2. Crystal structure of the HER3 kinase domain. (*A*) Structure of the HER3 kinase domain in complex with AMP-PNP is compared with the crystal structure of the inactive EGFR kinase domain in complex with AMP-PNP (PDB ID code 2GS7) and the inactive HER4 kinase domain (PDB ID code 3BBW). (*B*) Detailed view of helix αC in the structure of HER3 (purple) and inactive EGFR (gray). (*C*) Detailed view of the ATP-binding site in the HER3 kinase domain, showing the electron density (at 3.5 σ above the mean value) around the AMP-PNP molecule and the metal ion. The difference electron density maps shown were calculated using a model of the protein at a stage before the inclusion of the nucleotide in the refinement.

nally classified as a pseudokinase (13), we decided to reexamine whether the HER3 kinase domain has detectable kinase activity. The kinase domain of EGFR, lacking the juxtamembrane segment, has very low activity in solution (7, 21). The EGFR kinase domain can be activated by increasing its local concentration, which facilitates formation of the activating asymmetric dimer. This can be achieved by adding a polyhistidine tag to the kinase domain and concentrating it on the surface of small unilamellar vesicles containing lipids with nickel-nitrilotriacetic acid (Ni-NTA) lipid head groups to which the histidine-tagged kinase domains can bind (7).

We measured the rate of phosphate transfer by polyhistidine-tagged HER3 kinase domain toward a substrate peptide in the presence of such vesicles. In contrast to the EGFR kinase domain, the HER3 kinase domain has no detectable catalytic activity toward either a peptide derived from the sequence of a phosphorylation site on the EGFR (Fig. 3) or a generic tyrosine kinase substrate peptide, poly 4Glu:Tyr (Fig. S1), even when concentrated on vesicles. We tested the effects of divalent metals other than Mg^{2+} (i.e., Mn^{2+}, Ca^{2+}) on the activity of the kinase on lipid vesicles but did not detect measurable activity (Fig. S1). We also tested if the addition of EDTA, which is expected to remove metal ions from the protein, might increase HER3 kinase activity, as observed in the case of CASK (13). The addition of EDTA had no effect in the case of HER3 (Fig. S1).

Mutant forms of the EGFR kinase domain that cannot take the receiver position (the I682Q mutant) or the activator position (the V924R mutant) in the asymmetric dimer cannot be activated on vesicles (7). When these two mutant forms are mixed, activation on vesicles is restored. We measured the rate of phosphate transfer by the EGFR V924R mutant in the presence of the HER3 kinase domain. As shown in Fig. 3, HER3 is able to activate the EGFR V924R mutant. Disruption of the activator interface by mutating Val 926 in HER3 to arginine (corresponding to Val 924 in EGFR) blocks this effect (Fig. 3). Thus, although HER3 cannot function as a receiver kinase, it can play the role of an allosteric activator in the asymmetric dimer.

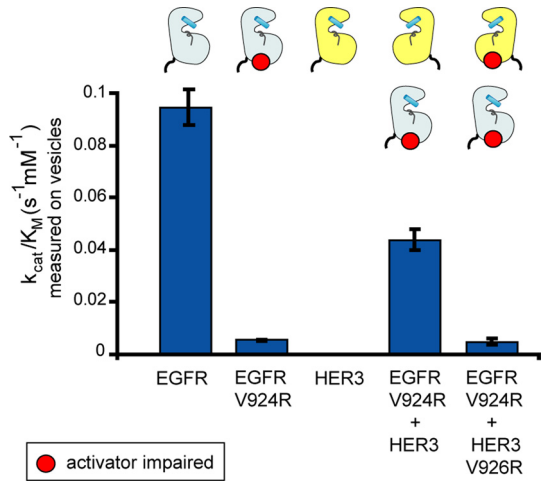

Fig. 3. HER3 is catalytically impaired as a receiver kinase but can function as an activator kinase. Catalytic efficiency (k_{cat}/K_M) of the kinase constructs (residues 672–998 in EGFR and residues 674–1,001 in HER3) on vesicles is measured using the continuous coupled-kinase assay. The values of k_{cat}/K_M were obtained from the linear dependence of reaction velocity on substrate concentration at a low substrate concentration, and the error bars are derived from the linear fit (7).

The Kinase Domains of HER3 and HER4 Form Similar Chains of Concatenated Dimers in Distinct Crystal Lattices. We noticed a set of interactions in the HER3 crystal lattice that generates an open-ended chain of kinase domains (Fig. 4*A*). The chain is best described as a linked set of dimers, in which the dimers are stabilized by close contacts between the N-lobes of pairs of kinase domains that are related to each other by a 180° rotation (the N-lobe dimer). One N-lobe dimer is linked to two other N-lobe dimers through interactions involving the C-terminal tails of the two kinase domains in the central dimer and the C-lobes of the adjacent kinase domains in the outer dimer (the C-lobe linkage).

The interface between kinase domains in the N-lobe dimer is tight and involves the juxtaposition of helices αC and portions of the juxtamembrane segments, with the burial of ~650 Å^2 of total surface area at the interface [calculated using the visual molecular dynamics (VMD) program (26)]. The interactions at the dimer interface are largely hydrophobic and involve residues Val 737 and Leu 742 from helix αC and Ile 684 from the juxtamembrane segment of the kinase domains (Fig. 4*B*). Remarkably, we found that the inactive HER4 kinase domain also forms a very similar N-lobe dimer [Protein Data Bank (PDB) ID codes 3BBT and 3BBW], although it crystallizes with different lattice symmetry (space group $P6_1$ for HER4 compared with C2 for the HER3 crystals) (Fig. 4 *A* and *B*) (27).

We aligned the HER3 and HER4 N-lobe dimers by least-square superposition of Cα atoms of the β-strands in the N-lobes. This results in a rms deviation in Cα-positions of 1.8 Å for the β-strands (because helix αC is distorted in HER3, it was excluded from the alignment), illustrating the structural similarity of the dimers (Fig. 4 *A* and *B*). The N-lobe dimer has additional potential significance for HER4 because its kinase domain can be activated, and the formation of this dimer would stabilize the inactive Src/CDK-like conformation rather than the active one.

We have evaluated the potential stability of the HER3 and HER4 N-lobe dimers over the course of long time-scale all-atom molecular dynamics simulations (see *SI Text* for details on the simulations). HER3 and HER4 N-lobe dimers were each simulated for 0.3 μs in an explicitly solvated environment, and the dimers were found not to dissociate over this time scale. Empirical estimation of the binding free energy for dimer formation was carried out using FoldX (28), with conformations sampled from the molecular

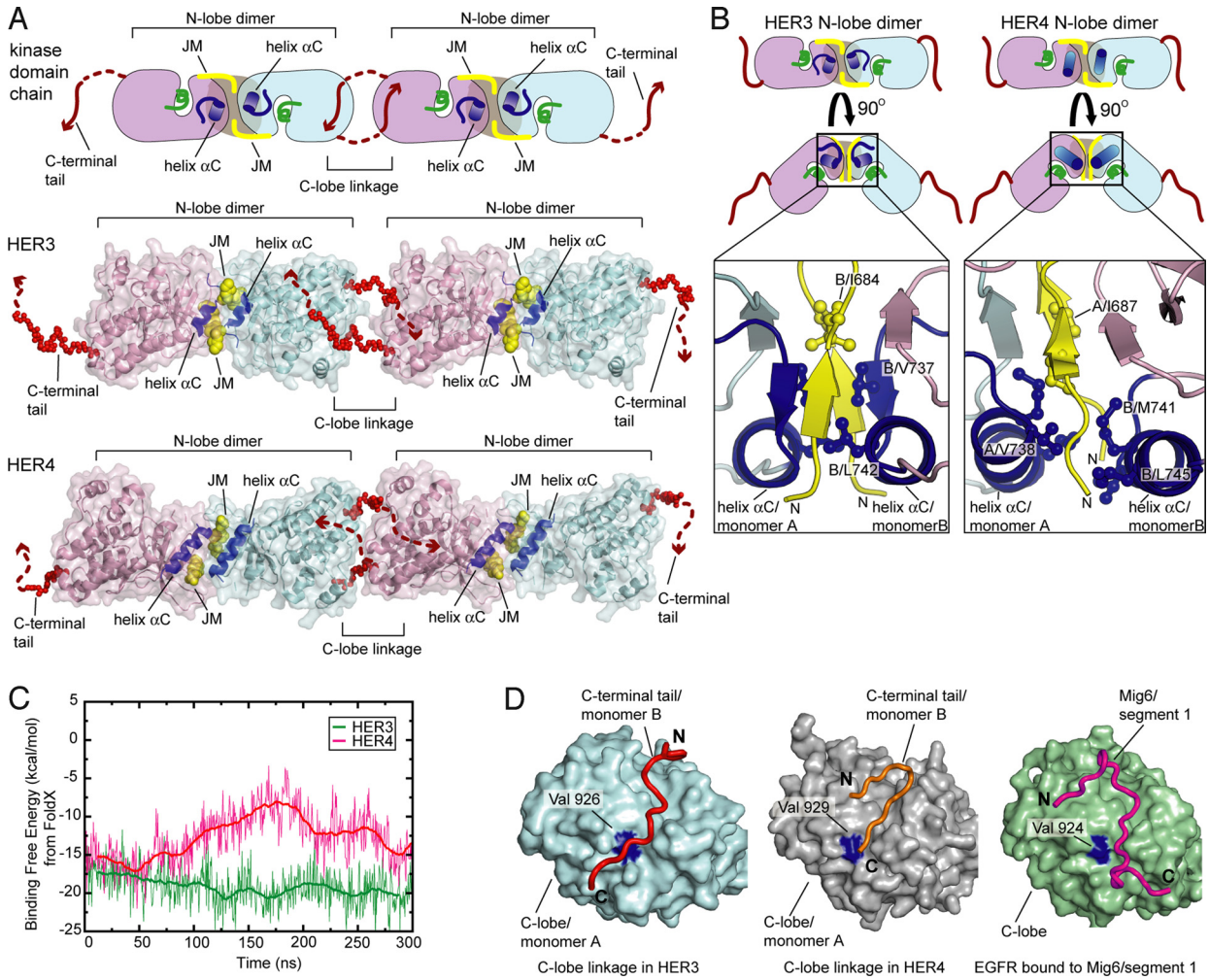

Fig. 4. Analysis of the concatenated HER3 and HER4 kinase domains in the crystal lattices. (*A*) Pattern of kinase monomer interactions observed in the crystal lattices of the kinase domains of HER3 and inactive HER4 (PDB ID code 3BBW). The C-terminal tail exchanging dimers are propagated through the N-lobe dimer interface. JM refers to portion of the juxtamembrane segment. (*B*) Detailed view of the HER3 and HER4 N-lobe dimers. Hydrophobic residues are shown in stick representation. (*C*) Empirical estimates of binding free energy of HER3 and HER4 N-lobe homodimers using conformations obtained from all-atom molecular dynamics simulations. (*D*) Comparison between the C-terminal tail interaction with the C-lobe in the HER3 kinase domain dimer and the HER4 kinase domain dimer (PDB ID code 3BBW) and interaction of Mig6/segment 1 with the C-lobe of the EGFR kinase domain (PDB ID code 2RFE).

dynamics trajectories. The estimated binding free energies remain negative over the course of simulation, and the dimer interface is largely protected from water penetration, suggesting that these two dimers represent stable complexes (Fig. 4*C* and Fig. S2 *A* and *B*). For comparison, we simulated another dimer observed in the HER3 crystal lattice, with a similar buried surface area (Fig. S3*A*), to which we do not attribute functional significance. In contrast to the N-lobe dimer, the other crystallographic dimer experiences extensive water penetration at the interface (Fig. S3*B*). This interface is also less stable, as judged by the higher FoldX binding energy and rms deviation in β-strand Cα-atoms over the course of the stimulations (Fig. S3 *C* and *D*).

The N-lobe dimers are linked together in the chain through a reciprocal exchange of C-terminal tails. This interaction is seen in both the HER3 and HER4 crystal lattices and involves the C-terminal tail of one kinase domain interacting with the C-lobe of the adjacent kinase domain in the crystal lattice (Fig. 4*A*). This C-lobe linkage is quasisymmetrical, in that the second kinase domain positions its C-terminal tail to form similar interactions with the C-lobe of the first kinase. Contiguous electron density for the C-terminal tail (residues 959–975) is seen in one molecule in the HER3 crystal structure. In the other molecule, the path of the C-terminus is partially blocked by a lateral crystal contact that results in disordering of residues 970–975. The linker that connects the end of the C-lobe of the first kinase domain (residue 962) to the portion of the C-terminal tail that engages the second kinase domain (residue 965) is partially disordered in both HER3 and HER4, and therefore appears to be intrinsically flexible.

The core interaction between the C-lobe and the C-terminal tail involves residues in the activator interface of the activating asymmetric dimer, such as Val 926 (Val 924 in EGFR) (Fig. 4*D*). One segment of the C-terminal tail in HER3 (residues 967–974) adopts a polyproline type II helical conformation that positions two proline residues in this region, Pro 971 and Pro 973, such that they bracket Val 926. An analogous interaction with the C-lobe is made by a segment of a negative feedback inhibitor of EGFR, Mig6, which limits EGFR activation by blocking the formation of the asymmetric dimer (29). The analogy between the binding of Mig6 to the activator site in EGFR and the C-terminal tail/C-lobe interface in HER3 and HER4 dimers points to a possible inhibitory role for this interaction.

Potential Implications for the Oligomerization of HER3 and HER4. The nature of the linkages in the HER3 and HER4 chains is such that

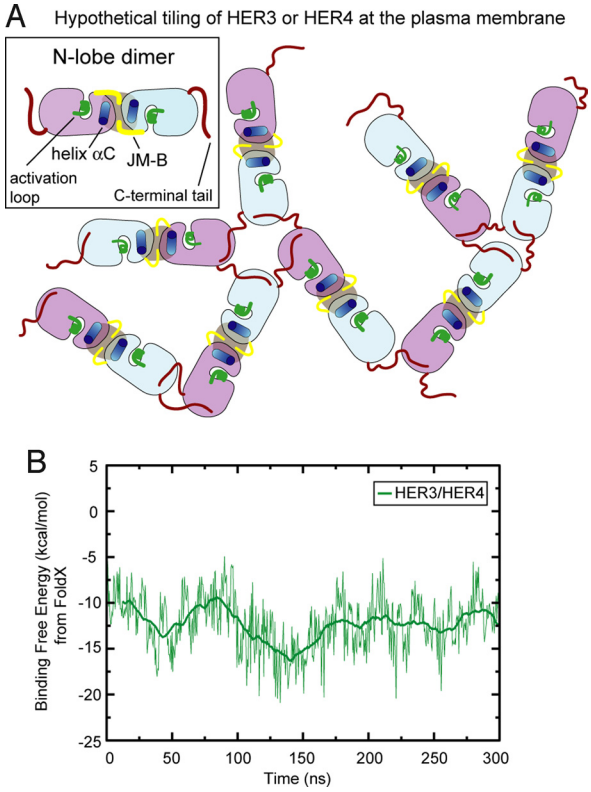

Fig. 5. Model for oligomerization of the kinase domains of HER3 and inactive HER4 at the plasma membrane. (*A*) Flexible C-terminal tail/C-lobe interaction creates a possibility for the formation of branched HER3 or inactive HER4 oligomers, resulting in a 2D mesh. (*B*) Empirical estimates of binding free energy of the HER3/HER4 N-lobe homodimer, calculated using conformations obtained from an all-atom molecular dynamics simulation.

if the chain were to run along the surface of a lipid bilayer, each N-lobe dimer would present the same face to the phospholipid head groups (Fig. S4*A*). Visualization of the surface electrostatic potential for the N-lobe dimer in HER3 shows that one face has predominantly positive electrostatic potential, whereas the opposite face does not. If the positively charged face is placed at the plasma membrane, the juxtamembrane segments are in a reasonable position for connection to the transmembrane segments (Fig. S4*A*). Thus, formation of these chains appears to be plausible in the context of the full-length receptor.

The flexibility of the C-terminal tail regions emerging from the kinase domains, as inferred by disorder in electron density maps, suggests that an exchange of C-terminal tails could occur between adjacent HER3 receptors without imposition of rigid geometry and without requiring that the tails be exchanged between just two N-lobe dimers. This may allow the assembly of branched chains, leading to the formation of a 2D tiling pattern of HER3 and HER4 at the plasma membrane (Fig. 5*A*).

The residues at the interface between N-lobe dimers are conserved between HER3 and HER4. This raises the possibility that the HER3 kinase domain might form heterodimers with that of inactive HER4. We modeled such a heterodimer by replacing one of the HER4 kinase domains in the HER4 N-lobe dimer with a HER3 kinase domain. We then estimated the free energy of binding using FoldX and sampling individual structures from a 0.3 μs molecular dynamics trajectory. This analysis suggests that HER3/HER4 N-lobe heterodimers may also be structurally stable (Fig. 5*B* and Fig S4*B*). One intriguing possibility is that the kinase domains of HER3 and HER4 might engage each other in a mutually inhibitory interaction before binding their common ligands, the neuregulins.

The HER3 and HER4 N-lobe dimers are quite distinct from a dimer of inactive EGFR kinase domains that has been described recently (21). The N-lobe dimers and the C-lobe linkages described above for HER3 and HER4 are not observed in any of the EGFR crystal lattices (the HER2 kinase domain has not yet been crystallized). The N-lobe dimer does not appear to be compatible with the EGFR sequence. Leu 742 in HER3 is located at the N-lobe interface and contributes to the stability of the interface in the molecular dynamics simulations. This residue is replaced by a tyrosine in EGFR. The presence of Lys 733 in helix αC of EGFR would introduce a positive charge at the mostly hydrophobic interface in the HER3/HER4 N-lobe dimers and may lead to the destabilization of the dimer. Notably, both Tyr and Lys residues at these positions are absent in mammalian HER3 and HER4 sequences but are present in HER2 (Fig. 1*B*). The portion of the C-terminal tail that has been visualized in crystal structures of the EGFR kinase domain does not make interactions that resemble the C-lobe linkages observed in the HER3 and HER4 crystal lattices. Thus, the chains of inactive kinase domains that we describe here may be unique to HER3 and HER4.

Concluding Remarks. The structure of the HER3 kinase domain shows that it is remarkably close to being a fully formed kinase domain but one that is locked into the inactive Src/CDK-like conformation. The HER3 kinase domain binds ATP and coordinates a metal ion in the active site, but this may be necessary to preserve the integrity of the structure rather than for a role in catalysis. We show that although the HER3 kinase domain is incapable of being a functional receiver kinase, it can indeed activate the EGFR kinase domain by formation of the asymmetric dimer. This result focuses attention on a key difference between the regulation of HER3 and other members of the EGFR family. For EGFR, HER2, and HER4, it is critical that their kinase activity be kept in check, and this is accomplished, at least in part, by autoinhibitory mechanisms that are released by ligand-induced dimerization. In contrast, the kinase domain of HER3 is always "active" in the sense that it has a C-lobe that is competent to engage and activate the kinase domains of the other members of the family.

One way in which HER3 is kept in check is through its sequestration in clusters in the absence of ligand (30, 31). Ligand binding to HER3 was shown to result in the dissociation of preexisting homooligomers of the extracellular domains of HER3, thereby enabling heterodimerization with HER2 and other EGFR family members (30–32). The identification of the chain of kinase domains in the crystal lattices of HER3, also found in HER4, provides a potential structural model that would explain why HER3 clustering might be inhibitory. In this model, the activator interface is occluded by C-terminal tails from adjacent kinase domains, which resembles, to some extent, the mechanism by which the Mig6 protein inhibits EGFR (29).

The conservation of the intermolecular interactions observed in the inactive structures of HER3 and HER4 suggests that they may share a common mechanism by which their activity is restricted in the absence of their shared activating ligands. That these intermolecular interactions may not be formed by the EGFR kinase domain may reflect the closer evolutionary ties between HER3 and HER4. Both HER3 and HER4 are postulated to originate from a gene duplication event distinct from the one that led to EGFR and HER2 (33). It is possible that by forming heterooligomers with each other, HER4 could limit the availability of HER3 as a dimerizing partner for HER2 when the activating ligand is not present. Such an interaction might explain the observation that in patients with breast cancer, where signaling from HER2/HER3 heterodimers is the driving force of tumor growth, HER4 overexpression is correlated with a favorable outcome

(34, 35). Future experiments will focus on unraveling the biological significance of these observations.

Materials and Methods

Protein Expression and Purification. DNA encoding residues 674–1,001 (numbering without the 19-aa signal peptide sequence) of human HER3 was cloned into pFAST BAC HT (Invitrogen), using the SfoI and XhoI restriction sites. The construct is flanked by an N-terminal 6-His tag and a cleavage site for the tobacco etch virus protease (TEV; MSYYHHHHHHDYDIPTTENLYFQGAM). For crystallization, the 6-His tag was cleaved off with TEV protease, which leaves the heterologous GAM peptide motif at the N- terminus of the HER3 kinase domain construct. Mutations were introduced using the Quick-Change kit (Stratagene) and confirmed by DNA sequencing.

The protein was expressed in Sf9 cells using the Bac-to-Bac expression system (Gibco BRL). Following expression, cells were harvested and homogenized by French press in resuspension buffer [50 mM Tris (pH 8.0), 5% vol/vol glycerol, 1 mM DTT]. The lysate was centrifuged at 40,000 $\times$ *g* for 1 h. The supernatant was loaded on a 60-mL Q Sepharose Fastflow column (Amersham) and equilibrated in buffer A [50 mM Tris (pH 8.0), 5% vol/vol glycerol, 15 mM β-mercaptoethanol]. The proteins were eluted using buffer B (buffer A plus 1 M NaCl) and loaded onto a 1-mL Histrap column (Amersham) equilibrated with buffer Ni-A [20 mM Tris (pH 8.0), 0.5 M NaCl, 5% vol/vol glycerol, 20 mM imidazole, 15 mM β-mercaptoethanol] and eluted with an imidazole gradient (20–250 mM). The proteins were then subjected to cleavage with TEV protease overnight, followed by purification using a 6-mL UnoQ column (Bio-Rad) equilibrated with buffer Q-A [20 mM Tris (pH 8.0), 20 mM NaCl, 5% vol/vol glycerol, 2 mM DTT]. The proteins were eluted with 20–500 mM NaCl gradient; concentrated; and buffer-exchanged into 20 mM Tris (pH 8.0), 50 mM NaCl, 2 mM DTT, and 2 mM tris(2-carboxyethyl)phosphine (TCEP). For the kinase assays, the TEV protease cleavage step was omitted.

Crystallization and Structure Determination. HER3 crystals were obtained initially from a solution containing HER3 kinase domains at 10 mg/mL, 5 mM AMP-PNP, 2 mM $MgCl_2$, 1 mM DTT, 1 mM TCEP, 0.1 M Tris (pH 8.5), 0.2 M lithium sulfate, 25% (wt/vol) PEG 3350, and diffracted x-rays to 7 Å. The crystals were further optimized using the Silver Bullets additive screen (Hampton Research), and diffraction data to 2.8-Å spacings were collected from crystals grown in the condition described above supplemented with 0.2% (wt/vol) 1,2-diaminocyclohexane sulfate, 0.2% (wt/vol) diloxanite furoate, 0.2% (wt/vol) fumaric acid, 0.2% (wt/vol) spermine, 0.2% (wt/vol) sulfaguanidine, and 0.02 M Hepes sodium (pH 6.8). Diffraction data were collected at −170 °C at ALS Beamline 8.2.1 and processed using the HKL2000 suite (36). The crystal structure was determined by molecular replacement using the structure of the EGFR V924R mutant in an inactive conformation as a search model (PDB ID code 2GS7) (7). The structure was refined using the Phenix refinement program (37) and by manual building using the O and Coot programs (38, 39).

In Vitro Kinase Assays. Kinase activity was measured using a continuous enzyme-coupled kinase assay on vesicles (7), utilizing a substrate peptide derived from the region corresponding to Tyr 1173 in EGFR (TAENAEYLRVAPQ) at a concentration of 1 mM or poly 4Glu:Tyr (Sigma) as a substrate at a concentration of 3 mg/mL. The kinase concentration in the assays was 7 μM. The reaction buffer contained 10 mM $MgCl_2$, 20 mM Tris (pH 7.5), and 0.5 mM ATP. The values of k_{cat}/K_M were derived from a linear fit to the substrate concentration dependence of the rates, using concentrations of the peptide that are much lower than the estimated value of K_M (7). To test the effect of other divalent metals and EDTA on kinase activity, 10 mM $MgCl_2$ in the reaction buffer was substituted with 10 mM $CaCl_2$, 10 mM $MnCl_2$, or 2 mM EDTA.

ACKNOWLEDGMENTS. We thank Chang Wang for technical help and Xuewu Zhang for the HER3 cDNA construct. We also thank Mark Moasser, Xuewu Zhang, and members of the Kuriyan laboratory for helpful discussions. This work was supported in part by Grant RO1 CA96504–06 from the National Cancer Institute (to J.K.) and by the Susan G. Komen Breast Cancer Foundation. We thank the staff at the Advanced Light Source, which is supported by the U.S. Department of Energy under Contract DE-AC03–76SF00098 at the Lawrence Berkeley National Laboratory.

1. Yarden Y, Sliwkowski MX (2001) Untangling the ErbB signalling network. *Nat Rev Mol Cell Biol* 2:127–137.
2. Guy PM, Platko JV, Cantley LC, Cerione RA, Carraway KL, 3rd (1994) Insect cell-expressed p180erbB3 possesses an impaired tyrosine kinase activity. *Proc Natl Acad Sci USA* 91:8132–8136.
3. Wieduwilt MJ, Moasser MM (2008) The epidermal growth factor receptor family: Biology driving targeted therapeutics. *Cell Mol Life Sci* 65:1566–1584.
4. Baselga J, Swain SM (2009) Novel anticancer targets: Revisiting ERBB2 and discovering ERBB3. *Nat Rev Cancer* 9:463–475.
5. Soltoff SP, Carraway KL, 3rd, Prigent SA, Gullick WG, Cantley LC (1994) ErbB3 is involved in activation of phosphatidylinositol 3-kinase by epidermal growth factor. *Mol Cell Biol* 14:3550–3558.
6. Sergina NV, et al. (2007) Escape from HER-family tyrosine kinase inhibitor therapy by the kinase-inactive HER3. *Nature* 445:437–441.
7. Zhang X, Gureasko J, Shen K, Cole PA, Kuriyan J (2006) An allosteric mechanism for activation of the kinase domain of epidermal growth factor receptor. *Cell* 125:1137–1149.
8. Jeffrey PD, et al. (1995) Mechanism of CDK activation revealed by the structure of a cyclinA-CDK2 complex. *Nature* 376:313–320.
9. Sierke SL, Cheng K, Kim HH, Koland JG (1997) Biochemical characterization of the protein tyrosine kinase homology domain of the ErbB3 (HER3) receptor protein. *Biochem J* 322:757–763.
10. Prigent SA, Gullick WJ (1994) Identification of c-erbB-3 binding sites for phosphatidylinositol 3′-kinase and SHC using an EGF receptor/c-erbB-3 chimera. *EMBO J* 13:2831–2841.
11. Wallasch C, et al. (1995) Heregulin-dependent regulation of HER2/neu oncogenic signaling by heterodimerization with HER3. *EMBO J* 14:4267–4275.
12. Manning G, Whyte DB, Martinez R, Hunter T, Sudarsanam S (2002) The protein kinase complement of the human genome. *Science* 298:1912–1934.
13. Mukherjee K, et al. (2008) CASK functions as a Mg2+-independent neurexin kinase. *Cell* 133:328–339.
14. Scheeff ED, Eswaran J, Bunkoczi G, Knapp S, Manning G (2009) Structure of the pseudokinase VRK3 reveals a degraded catalytic site, a highly conserved kinase fold, and a putative regulatory binding site. *Structure* 17:128–138.
15. De Bondt HL, et al. (1993) Crystal structure of cyclin-dependent kinase 2. *Nature* 363:595–602.
16. Sicheri F, Moarefi I, Kuriyan J (1997) Crystal structure of the Src family tyrosine kinase Hck. *Nature* 385:602–609.
17. Xu W, Doshi A, Lei M, Eck MJ, Harrison SC (1999) Crystal structures of c-Src reveal features of its autoinhibitory mechanism. *Mol Cell* 3:629–638.
18. Deindl S, et al. (2007) Structural basis for the inhibition of tyrosine kinase activity of ZAP-70. *Cell* 129:735–746.
19. Wood ER, et al. (2004) A unique structure for epidermal growth factor receptor bound to GW572016 (Lapatinib): Relationships among protein conformation, inhibitor off-rate, and receptor activity in tumor cells. *Cancer Res* 64:6652–6659.
20. Huse M, Kuriyan J (2002) The conformational plasticity of protein kinases. *Cell* 109:275–282.
21. Jura N, et al. (2009) Mechanism for activation of the EGF receptor catalytic domain by the juxtamembrane segment. *Cell* 137:1293–1307.
22. Red Brewer M, et al. (2009) The juxtamembrane region of the EGF receptor functions as an activation domain. *Mol Cell* 34:641–651.
23. Cho HS, Leahy DJ (2002) Structure of the extracellular region of HER3 reveals an interdomain tether. *Science* 297:1330–1333.
24. Levinson NM, et al. (2006) A Src-like inactive conformation in the abl tyrosine kinase domain. *PLoS Biol* 4:e144.
25. Shan Y, et al. (2009) A conserved protonation-dependent switch controls drug binding in the Abl kinase. *Proc Natl Acad Sci USA* 106:139–144.
26. Humphrey W, Dalke A, Schulten K (1996) VMD: Visual molecular dynamics. *J Mol Graphics* 14:33–38.
27. Qiu C, et al. (2008) Mechanism of activation and inhibition of the HER4/ErbB4 kinase. *Structure* 16:460–467.
28. Schymkowitz J, et al. (2005) The FoldX web server: An online force field. *Nucleic Acids Res* 33(Web Server issue):W382–W388.
29. Zhang X, et al. (2007) Inhibition of the EGF receptor by binding of MIG6 to an activating kinase domain interface. *Nature* 450:741–744.
30. Landgraf R, Eisenberg D (2000) Heregulin reverses the oligomerization of HER3. *Biochemistry* 39:8503–8511.
31. Kani K, Park E, Landgraf R (2005) The extracellular domains of ErbB3 retain high ligand binding affinity at endosome pH and in the locked conformation. *Biochemistry* 44:15842–15857.
32. Berger MB, Mendrola JM, Lemmon MA (2004) ErbB3/HER3 does not homodimerize upon neuregulin binding at the cell surface. *FEBS Lett* 569:332–336.
33. Stein RA, Staros JV (2006) Insights into the evolution of the ErbB receptor family and their ligands from sequence analysis. *BMC Evol Biol* 6:79.
34. Barnes NL, et al. (2005) Absence of HER4 expression predicts recurrence of ductal carcinoma in situ of the breast. *Clin Cancer Res* 11:2163–2168.
35. Kew TY, et al. (2000) c-erbB-4 protein expression in human breast cancer. *Br J Cancer* 82:1163–1170.
36. Otwinowski Z, Minor W (1997) Processing of x-ray diffraction data collected in oscillation mode. *Methods Enzymol* 276:307–326.
37. Adams PD, et al. (2002) PHENIX: Building new software for automated crystallographic structure determination. *Acta Crystallogr D* 58(Pt 11):1948–1954.
38. Jones TA, Zou JY, Cowan SW, Kjeldgaard M (1991) Improved methods for building protein models in electron density maps and the location of errors in these models. *Acta Crystallogr A* 47(Pt 2):110–119.
39. Emsley P, Cowtan K (2004) Coot: Model-building tools for molecular graphics. *Acta Crystallogr D* 60(Pt 12 Pt 1):2126–2132.